Analysis of Cell Mechanics in Single Vinculin-Deficient Cells Using a Magnetic Tweezer

Francis J. Alenghat,* Ben Fabry,† Kenneth Y. Tsai,*
Wolfgang H. Goldmann,* and Donald E. Ingber*,1

*Department of Pathology and Department of Surgery, Children's Hospital and Harvard Medical School, Boston, Massachusetts 02115; and †Physiology Program, Harvard School of Public Health, Boston, Massachusetts 02115

A magnetic tweezer was constructed to apply controlled tensional forces (10 pN to greater than 1 nN) to transmembrane receptors via bound ligand-coated microbeads while optically measuring lateral bead displacements within individual cells. Use of this system with wild-type F9 embryonic carcinoma cells and cells from a vinculin knockout mouse F9 Vin (−/−) revealed much larger differences in the stiffness of the transmembrane integrin linkages to the cytoskeleton than previously reported using related techniques that measured average mechanical properties of large cell populations. The mechanical properties measured varied widely among cells, exhibiting an approximately log-normal distribution. The median lateral bead displacement was 2-fold larger in F9 Vin (−/−) cells compared to wild-type cells whereas the arithmetic mean displacement only increased by 37%. We conclude that vinculin serves a greater mechanical role in cells than previously reported and that this magnetic tweezer device may be useful for probing the molecular basis of cell mechanics within single cells.   © 2000 Academic Press

Key Words: **mechanical stress; integrin; vinculin; mechanotransduction; focal adhesion; magnetometry.**

Control of cell mechanics and shape is crucial for many cellular functions, including growth, differentiation, migration, and gene expression (1–6). The mechanical properties of the cell, in turn, are established through a balance of mechanical forces: tension generated by actin filaments is counteracted by compression-resistant extracellular matrix (ECM) anchors as well as internal microtubule struts (7–10). Any alteration in cell mechanics may therefore change the cell's internal molecular structure and thereby alter cellular biochemistry (11, 12). Consequently, many investigators seek to analyze the mechanical properties of cells by applying controlled stresses to living cells and recording the mechanical response. Techniques previously employed to apply controlled mechanical stresses to cell surfaces include: micropipette aspiration (13–15), cell poking (16–18), deformable culture substrates (19, 20), and fluid shear stresses (8, 21–23). All of these methods, however, lack molecular specificity in their manner of stress application; they either distort whole cells or large areas of cell membrane.

Forces applied to the cell surface are preferentially transmitted across the membrane and to the cytoskeleton through integrins which cluster within localized ECM binding sites (focal adhesions) (11, 24). Other mechanical manipulation techniques have therefore been developed to apply mechanical stresses specifically to transmembrane integrin receptors and their associated cytoskeletal proteins. These methods include use of either optical tweezers (25, 26), magnetic twisting forces (24, 27), or magnetic dragging forces (28) to manipulate surface-bound microbeads coated with integrin receptor ligands. Optical tweezers can be used to pull on integrins on individual living cells, but they are limited to forces in the low piconewton (pN) range, and thus they cannot measurably deform the cell after focal adhesions and associated strong connections between integrins and the cytoskeleton have formed (26, 29). Magnetic twisting cytometry (MTC) offers the ability to apply much larger forces (up to ~500 pN) and thus, to probe deeply into the cell, even after focal adhesions have formed. However, MTC requires that tens of thousands of cells be measured simultaneously in order to sense the average bead rotation in response to application of a magnetic torque. Because MTC only measures a population average, it may therefore obscure important behaviors of individual cells.

¹ To whom correspondence should be addressed at Department of Pathology and Department of Surgery, Enders 1007, Children's Hospital, 300 Longwood Avenue, Boston, MA 02115. Fax: (617) 232-7914. E-mail: ingber@a1.tch.harvard.edu.
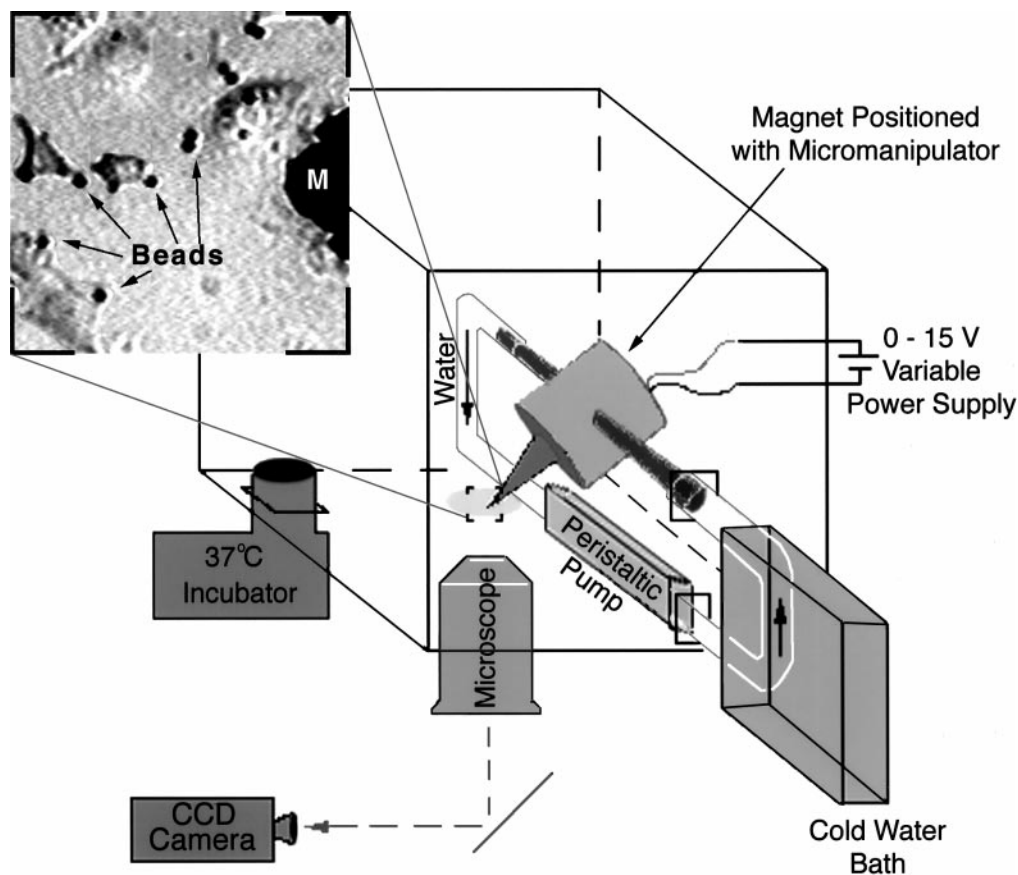
FIG. 1. Diagram of the magnetic tweezer. The goal of the magnetic tweezer technique is to arrange a small "tug-of-war" between the electromagnet and the cell. The magnet is mounted on a micromanipulator secured to a light microscope, with the entire working area heated to 37°C and cold water circulating through the brass housing of the magnet to prevent overheating of the wire as high current passes through it. A microscopic view (inset) of the area on the coverslip shows the beads (4.5 μm diameter) bound to the surfaces of cultured cells relative to the position of the tip of the magnet (M).

In the present study, we constructed a magnetic tweezer based on the modification of a previously described device (30) which permits us to quantitate mechanical properties of individual living cells in response to application of a wide range of mechanical tension (from pN to nN forces). These tensile stresses are applied to specific cell surface integrin receptors using the same ligand-coated magnetic microbeads that are utilized in MTC. These beads have been previously characterized in detail in terms of their ability to bind integrins with high specificity and to induce focal adhesion formation (31). To determine the value of this technique, we measured the mechanical properties of F9 embryonic carcinoma cells from a vinculin knockout mouse F9 Vin (−/−) which have been previously shown to exhibit a 21% decrease in stiffness relative to wild-type F9 cells when measured with MTC (32). Here we show that because cells exhibit a log-normal distribution of mechanical properties when measured individually using the magnetic tweezer, a much larger (more than 2-fold) difference in stiffness

could be detected in F9 Vin (−/−) cells relative to wild-type cells.

MATERIALS AND METHODS

Experimental system. Wild-type F9 and F9 Vin (−/−) mouse embryonic cells were maintained on tissue-culture treated plastic dishes in high glucose (4.5 g/L) Dulbecco's modified Eagle's medium with 10% calf serum, 20 mM Hepes, and 100 U/ml GPS (penicillin-streptomycin), as previously described (33). Cultured cells were trypsinized and plated in fresh medium for 12 h on 35 mm circular petri dishes with a glass coverslip bottom (Mattek) coated with 500 ng/cm^2 fibronectin before adding magnetic beads. Tosyl-activated superparamagnetic beads (4×10^7 Dynabeads/ml; 4.5 μm diameter; Dynal) were coated with a synthetic RGD-containing peptide (Peptite-2000; Integra) in phosphate buffer solution and added to cultured cells (2×10^5 beads/ml), as previously described (24). The cells were incubated for 30 min before the cells were washed free of unbound beads and magnetic pulling was initiated.

Magnetic tweezer. To construct the magnetic tweezer, a thousand turns of 30 gauge copper wire were wound around the shaft of a pole (6 cm long, 0.5 cm diameter shaft, 30 μm diameter tip) made from a magnetic alloy, HyMu 80 (Carpenter, Reading, PA). The shaft and coils were enclosed in a brass housing from which the wire leads,

water inlet and outlet, and pole tip protrude (Fig. 1). The wire leads were connected to a variable power source that provided a potential difference between 1.0 and 15 V. The resistance of the coiled wire was 10 Ω; this corresponds to currents ranging from 0.1 to 1.5 amperes (amp).

The force applied to each magnetic bead is a function of the distance between the bead and the tip of the electromagnet. It also depends on the current through the magnet and the mass and magnetic mass susceptibility of the beads (in this case, 16×10^{-5} m³/kg). The magnetic tweezer was calibrated by pulling the 4.5 μm diameter beads through a glycerol solution with a known high viscosity (1 kg/m/s, or 1000 centipoise). After recording the beads' velocities through the fluid, Stokes' Formula for low Reynolds number flow was used to deduce the forces. [Force = $3\pi\eta Dv$, where η is the viscosity of the fluid; D is the bead diameter, and v is the velocity of the bead through the fluid.] The magnet tip was positioned less than 5 μm above the coverslip (within the liquid medium). When the electromagnet was turned on, the beads migrated toward the magnet tip and displacements were quantitated using a video camera and IPLab image analysis software; bead velocity was then plotted against the distance from the tip. Using Stokes' Law, the force on the bead was deduced from its velocity and thus, a force versus distance relationship could be determined for various driving currents.

Cell pulling. Cells with bound beads were maintained at 37°C on a Nikon Diaphot microscope stage and positioned at a distance of 300 μm from the tip of the magnet. A still image was captured through a DAGE MTI CCD camera using the Apple Video Player frame grabber for Macintosh. The magnet was then turned on at 1.0 amp current to produce a force of 180 pN on each bead bound to the cell; after 5 s another still image was captured. The current through the magnet was then returned to zero, and five seconds later, a third image was captured. This triplet of OFF–ON–OFF images was used to obtain a value for bead displacement and recoil in response to magnetic stress application and release. A Matlab image analysis program calculated these bead positions with subpixel resolution. This procedure was then repeated with multiple cells per dish, always ensuring that the distance between the different regions examined was significantly large (>3 mm) to be sure that the next cell examined had not experienced any significant force from the previous measurements.

RESULTS AND DISCUSSION

This work was initiated to explore whether a magnetic tweezer (Fig. 1) would be useful for noninvasive analysis of cell mechanics, and in particular, for quantitation of changes in the mechanics of the integrin–cytoskeleton linkage that result from alterations in the expression of specific cytoskeletal proteins within single cells. Calibration studies carried out using the magnetic tweezer to pull beads through a high viscosity (1000 centipoise) glycerol solution resulted in the development of reproducible force–distance relationships for the different currents used in these studies (Fig. 2). By varying the current and the distance from the tip, forces ranging from a few pN to in excess of 1 nN could be applied to 4.5 μm magnetic beads. However, when high forces were applied at low currents (0.1 or 0.5 amp), the measured force changed drastically with distance and thus, small variations in distance could significantly alter the level of force applied. In our studies, we therefore used a higher current (1 amp) to drive the magnet, which displays a more linear relationship between force and distance and maintains significant
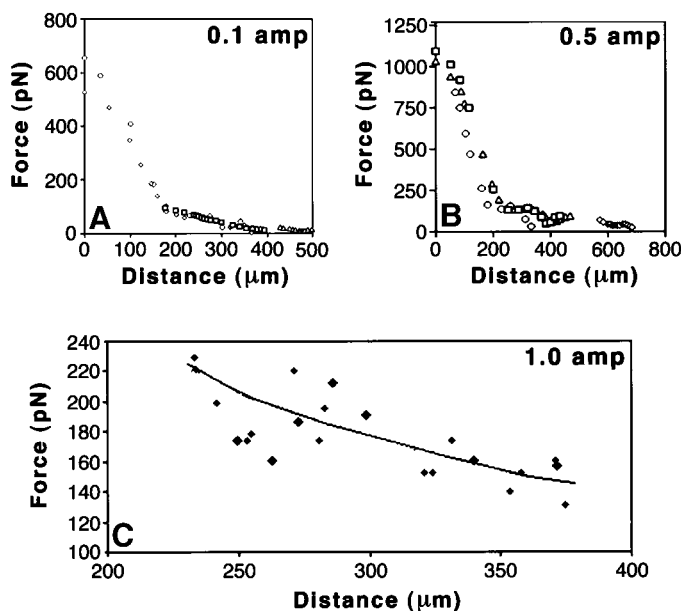

FIG. 2. Calibration of the magnetic tweezer. The relationships between distance and force for application of currents through the magnet of 0.1 (A), 0.5 (B), and 1 (C) amp. Differently shaped data points refer to distinct beads as their journey toward the magnet tip was tracked. Note that the force on a bead could be tuned from a few pN to in excess of a nN. The magnetic tweezer was driven with 1 amp in all subsequent experiments and the tip of the magnet was held at 300 μm from the pole tip; this corresponds to a force of approximately 180 pN being experienced by beads.

levels of force (150 to 225 pN) over a wide range of distance.

In all experiments, the beads analyzed were 300 μm from the tip of the magnet; at 1 amp, this corresponds to a pulling force of 180 pN (Fig. 2C). With this level of stress application, bead displacement was minute, but sometimes discernable as a slight jump toward the magnet. The Matlab image analysis program, however, is able to resolve even very small displacements with an accuracy (rms) of 20 nm. Subtraction of images recorded before (Fig. 3A) and after stress application to cells revealed displacement of the beads in response to magnetic tension as a thin white crescent on a black background (Fig. 3B).

The magnetic tweezer was constructed with the goal of applying focused and quantifiable mechanical stress to individual cells in culture, perhaps revealing mechanical characteristics not readily discernable in traditional cell population studies. We examined vinculin-deficient F9 cells because the population-based properties of these cells are well characterized (32, 33) and thus, they serve as benchmarks with which the results of the present study may be compared. When a large number of individual wild-type [*n* = 213] and Vin (−/−) [*n* = 246] F9 cells were analyzed, we found that the number of beads that completely detached from cells upon stress application
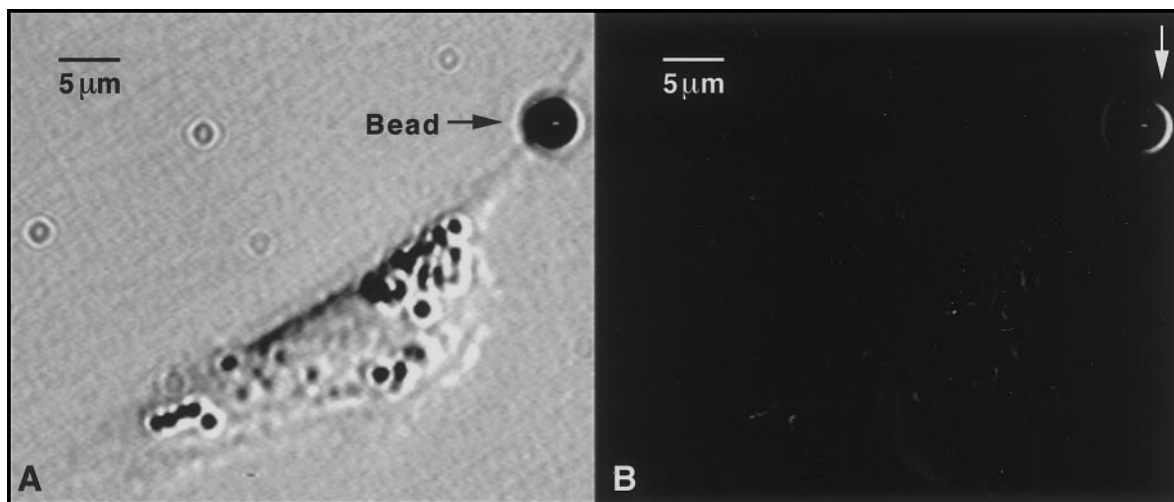
FIG. 3. Visualization of bead displacement using computerized image processing. The forces applied to the magnetic beads using the magnetic tweezer produced visually discernable displacements when the beads were coated with RGD-peptide and bound to cell surface integrins. (A) A bright-field image of a Vin (−/−) F9 cell with a bead bound to its surface at the top right of the view. (B) A composite digital image created from the image shown in A by subtracting a second image (not shown) of the same cell taken 5 s after application of 180 pN of stress through the magnetic tweezer. The tip of the magnet is positioned 300 μm to the right and is not visible in this view. The displacement of the bead to the right in response to the applied force (approximately 1 μm in this study) appears as a white crescent on the right edge of the bead (white arrow). Exact measurements of bead displacements, however, were obtained using a computerized pixel analysis algorithm.

was similar and low in both cells (5.2% and 4.5%, respectively). These results confirm that the cells' binding affinities for the RGD-beads were both strong and thus, that the absence of vinculin did not significantly interfere with the initial integrin binding interactions or recruitment of other focal adhesion proteins to the bead binding site, as previously demonstrated (32, 33).

Importantly, using this novel magnetic tweezer technique that permits cell-by-cell analysis, we discovered that the distribution of bead displacements was wide in both cell types (Figs. 4A and 4B). The data also demonstrated a skewed distribution when a linear scale was utilized, whereas a normal distribution appeared when plotted on a log-scale. This log-normal distribution was observed regardless of vinculin's presence or absence and similar results were obtained with another cell type (endothelial cells) using this method. The displacement in response to a fixed force of 180 pN ranged from less than 10 nm to above 1 μm (Fig. 4B). This large variation in bead displacement could not be accounted for by differences in bead binding time since all beads were allowed to bind for 30 min prior to a pulling trial. Moreover, beads that were pulled later in an experiment did not appear to displace less.

Analysis of the log-normal distribution revealed that the median displacement for the vinculin-deficient cells was double that of the wild-type cells (120 nm versus 60 nm) whereas the mean was only 37% greater for the Vin (−/−) cells (Fig. 4C). This latter result is similar to that previously obtained in the same cells using MTC, which measures population averages (32). The fact that the difference between medians is signif-

icantly greater than that between the means indicates that the displacements of the wild-type cells were more positively skewed than those of the Vin (−/−) cells. Because average bead displacement is dominated by only a few beads with large displacements, the median gives a more representative value for all beads.

Given that vinculin normally serves to physically interconnect integrins to internal cytoskeletal elements within the FAC, it is not surprising that the vinculin-deficient cells exhibited a major increase in bead displacement and thus, a major decrease in mechanical stiffness (median of approximately 1.5×10^{-3} N/m compared to 3.0×10^{-3} N/m for wild-type cells, as estimated based on pure elasticity), when measured through integrins (Fig. 4). In fact, the larger effect (2-fold increase in displacements) measured by individual cell analysis used in the present study is much more consistent with vinculin playing a major role as a stabilizer of focal adhesion structure, as suggested by the biochemical and cell biological literature (34, 35), than the much smaller difference (approximately 21% decrease in stiffness) obtained with MTC (32). The structural importance of vinculin may actually be underestimated by these measurements since previous studies have shown that other focal adhesion proteins are up-regulated in the Vin (−/−) cells (36). The existence of alternative load-bearing connections between integrins and the cytoskeleton in the vinculin-deficient cells was also demonstrated by the fact that very few beads became detached from the surface when large stresses were applied to beads bound to integrins on the surface of these cells. In contrast, application of
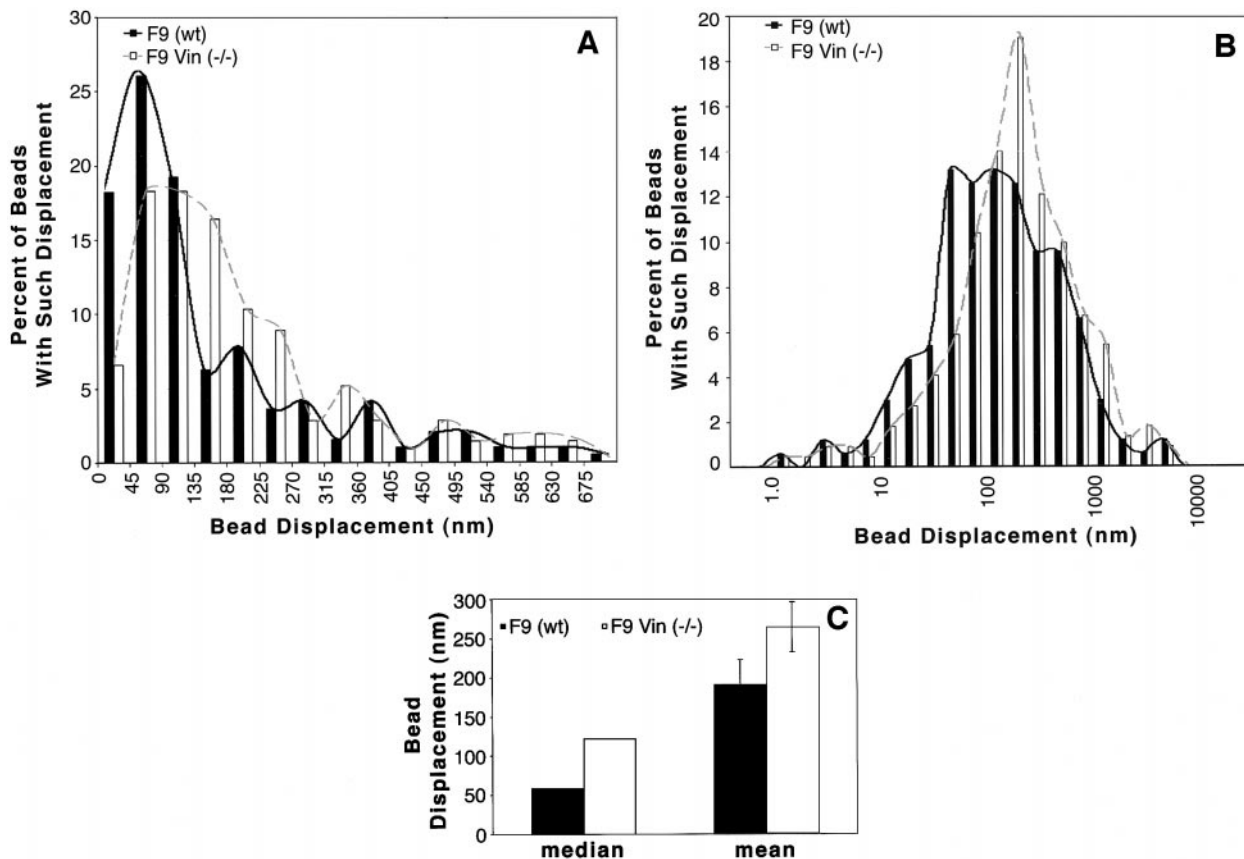
FIG. 4. Bead displacements in response to stress application in wild-type versus Vin (−/−) F9 cells measured with the magnetic tweezer. Histographs plotted on linear (A) versus log (B) scales show the distribution of bead displacements in response to application of a force of 180 pN to cell surface-bound RGD-beads. The bead displacements were distributed over a wide range, as evidenced by their almost normal distribution on a log scale, with geometric standard deviations of 3.9 and 4.1 for Vin (−/−) and wild-type, respectively (B). The median and mean displacements measured for wild-type versus Vin (−/−) F9 cells are shown in C. The vinculin-deficient cells exhibited a median bead displacement approximately double that of their wild-type counterparts (122 nm vs 59 nm, respectively) whereas mean displacement only increased by about 37% (265 nm vs 193 nm, respectively).

similar forces to beads coated with a ligand for cell surface metabolic receptors (acetylated low-density lipoprotein) exhibited much larger displacements, and beads were easily pulled off the cells with the magnetic tweezer (data not shown). The fact that a log-normal distribution of bead displacements was observed independent of the presence or absence of vinculin and in different cell types also suggests that the local mechanical properties of cells may be highly dependent on the local structure of individual focal adhesions. In fact, past immunofluorescent analysis of recruitment of different cytoskeletal proteins to the focal adhesion in response to binding of RGD-coated microbeads revealed significant differences in the composition of individual focal adhesion complexes (31, 37, 38). For example, while most focal adhesions in endothelial cells recruited talin 30 min after bead binding, less than 50% exhibited vinculin at a similar time (37).

Displacements of cell surface-bound beads coated with integrin ligands have previously been analyzed using another form of magnetic tweezer (30), but the wide range of displacements in response to force observed in the present study was not noted. This may be because only 10 cells were examined in total in that study. However, the authors did mention that viscoelastic parameters may differ by up to an order of magnitude from cell to cell, whereas values obtained for each individual cell differed by much less. In contrast, our results obtained with a much larger cell sampling number (hundreds of cells) indicate that this range is, in fact, much greater than an order of magnitude, that it is log-normally distributed, and that mechanical values also can differ greatly between different beads on the same cell. In any case, the present results indicate that examining cell mechanics on an individual cell basis using the magnetic tweezer technique reveals novel aspects of the material properties of the integrin–cytoskeleton linkage that are obscured in studies, such as those involving MTC (32), which are based on analysis of large cell populations.

ACKNOWLEDGMENTS

REFERENCES

1. Folkman, J., and Moscona, A. (1978) Role of cell shape in growth control. *Nature* **273,** 345–349.

2. Ingber, D. E. (1990) Fibronectin controls capillary endothelial cell growth by modulating cell shape. *Proc. Natl. Acad. Sci. USA* **87,** 3579–3583.

3. Mooney, D., Hansen, L., Farmer, S., Vacanti, J., and Ingber, D. E. (1992) Switching from differentiation to growth in hepatocytes: Control by extracellular matrix. *J. Cell. Physiol.* **151,** 497–505.

4. Singhvi, R., Kumar, A., Lopez, G. P., Stephanopoulos, G. N., Wang, D. I. C., Whitesides, G. M., and Ingber, D. E. (1994) Engineering cell shape and function. *Science* **264,** 696–698.

5. Chen, C. S., Mrksich, M., Huang, S., Whitesides, G. M., and Ingber, D. E. (1997) Geometric control of cell life and death. *Science* **276,** 1425–1428.

6. Meyer, C. J., Alenghat, F. J., Rim, P., Fong, J. H., Fabry, B., and Ingber, D. E. (2000) Mechanical control of cyclic AMP signalling and gene transcription through integrins. *Nat. Cell Biol.* **2,** 666–668.

7. Sims, J. R., Karp, S., and Ingber, D. E. (1992) Altering the cellular mechanical force balance results in integrated changes in cell, cytoskeletal, and nuclear shape. *J. Cell Sci.* **103,** 1215–1222.

8. Barbee, K. A., Davies, P. F., and Lal, R. (1994) Shear stress-induced reorganization of the surface topography of living endothelial cells imaged by atomic force microscopy. *Circ. Res.* **74,** 163–171.

9. Puck, T. T., and Krystosek, A. (1992) Role of the cytoskeleton in genome regulation and cancer. *In* International Review of Cytology (Jeon, K. W., and Friedlander, M., Eds.), pp. 75–108, Academic Press, San Diego, CA.

10. Ingber, D. E. (1993) The riddle of morphogenesis: A question of solution chemistry or molecular cell engineering? *Cell* **75,** 1249–1252.

11. Ingber, D. E. (1991) Integrins as mechanochemical transducers. *Curr. Opin. Cell Biol.* **3,** 841–848.

12. Ingber, D. E. (1993) Cellular tensegrity: Defining new rules of biological design that govern the cytoskeleton. *J. Cell Sci.* **104,** 613–627.

13. Schmid-Schonbein, G. W., Sung, K.-L. P., Tozeren, H., Skalak, R., and Chien, S. (1981) Passive mechanical properties of human leukocytes. *Biophys. J.* **36,** 243–256.

14. Hochmuth, R. M., and Waugh, R. E. (1987) Erythrocyte membrane elasticity and viscosity. *Annu. Rev. Physiol.* **49,** 209–219.

15. Evans, E., and Yeung, A. (1989) Apparent viscosity and cortical tension of blood granulocytes determined by micropipet aspiration. *Biophys. J.* **56,** 151–160.

16. Daily, B., Elson, E. L., and Zahalak, G. I. (1984) Cell poking. Determination of the elastic area compressibility modulus of the erythrocyte membrane. *Biophys. J.* **45,** 671–682.

17. Duszyk, M., Schwab, B., Zahalak, G. I., Qian, H., and Elson, E. L. (1989) Cell poking: Quantitative analysis of indentation of thick viscoelastic layers. *Biophys. J.* **55,** 683–690.

18. Goldmann, W. H. (2000) Mechanical manipulation of animal cells: Cell indentation. *Biotech. Lett.* **22,** 431–435.

19. Sumpio, B. E., and Banes, A. J. (1988) Response of porcine aortic smooth muscle cells to cyclic tensional deformation in culture. *J. Surg. Res.* **44,** 696–701.

20. Vandenburgh, H. H., Swasdison, S., and Karlisch, P. (1991) Computer-aided mechanogenesis of skeletal muscle organs from single cells in vitro. *FASEB J.* **5,** 2860–2867.

21. Levesque, M. J., and Nerem, R. M. (1989) The study of rheological effects on vascular endothelial cells in culture. *Biorheology* **26,** 345–357.

22. Davies, P. F., and Tripathi, S. C. (1993) Stress mechanisms in cultured cells: An endothelial paradigm. *Circ. Res.* **72,** 239–245.

23. Bhullar, I. S., Li, Y. S., Miao, H., Zandi, E., Kim, M., Shyy, J. Y-J., and Chien, S. (1998) Fluid shear stress activation of IκB kinase is integrin-dependent. *J. Biol. Chem.* **273,** 30544–30549.

24. Wang, N., Butler, J. P., and Ingber, D. E. (1993) Mechanotransduction across the cell surface and the cytoskeleton. *Science* **260,** 1124–1127.

25. Kuo, S. C., and Sheetz, M. P. (1993) Force of single kinesin molecules measured with optical tweezers. *Science* **260,** 232–234.

26. Maniotis, A. J., Chen, C. S., and Ingber, D. E. (1997) Demonstration of mechanical connections between integrins, cytoskeletal filaments, and nucleoplasm that stabilize nuclear structure. *Proc. Natl. Acad. Sci. USA* **94,** 849–854.

27. Wang, N., and Ingber, D. E. (1994) Control of cytoskeletal mechanics by extracellular matrix, cell shape, and mechanical tension. *Biophys. J.* **66,** 2181–2189.

28. Bausch, A. R., Moller, W., and Sackmann, E. (1999) Measurement of local viscoelasticity and forces in living cells by magnetic tweezers. *Biophys. J.* **76,** 573–579.

29. Schmidt, C. E., Dai, J., Lauffenburger, D. A., Sheetz, M. P., and Horwitz, A. F. (1995) Integrin–cytoskeletal interactions in neuronal growth cones. *J. Neurosci.* **15,** 3400–3407.

30. Bausch, A. R., Ziemann, F., Boulbitch, A. A., Jacobson, K., and Sackmann, E. (1998) Local measurements of viscoelastic parameters of adherent cell surfaces by magnetic bead microrheometry. *Biophys. J.* **75,** 2038–2049.

31. Plopper, G. E., McNamee, H. P., Dike, L. E., Bojanowski, K., and Ingber, D. E. (1995) Convergence of integrin and growth factor receptor signaling pathways within the focal adhesion complex. *Mol. Biol. Cell* **6,** 1349–1365.

32. Goldmann, W. H., Galneder, R., Ludwig, M., Xu, W., Adamson, E. D., Wang, N., and Ezzell, R. M. (1998) Differences in elasticity of vinculin-deficient F9 cells measured by magnetometry and atomic force microscopy. *Exp. Cell Res.* **239,** 235–242, doi: 10.1006/excr.1997.3915.

33. Ezzell, R. M., Goldmann, W. H., Wang, N., Parasharama, N., and Ingber, D. E. (1997) Vinculin promotes cell spreading by mechanically coupling integrins to the cytoskeleton. *Exp. Cell Res.* **231,** 14–26, doi:10.1006/excr.1996.3451.

34. Johnson, R. P., and Craig, S. W. (1995) F-actin binding site masked by the intramolecular association of vinculin head and tail domains. *Nature* **373,** 261–264.

35. Gilmore, A. P., and Burridge, K. (1996) Regulation of vinculin binding to talin and actin by phosphatidyl-inositol-4-5-bisphosphate. *Nature* **381,** 531–535.

36. Volberg, T., Geiger, B., Kam, Z., Pankov, R., Simcha, I., Sa-

banay, H., Coll, L. J., Adamson, E. D., and Ben-Ze'ev, A. (1995) Focal adhesion formation by F9 embryonal carcinoma cells after vinculin gene disruption. *J. Cell Sci.* **108,** 2253–2260.

37. Plopper, G., and Ingber, D. E. (1993) Rapid induction and isola-

tion of focal adhesion complexes. *Biochem. Biophys. Res. Commun.* **193,** 571–578, doi:10.1006/bbrc.1993.1662.

38. Miyamoto, S., Akiyama, S. K., and Yamada, K. M. (1995) Synergistic roles for receptor occupancy and aggregation in integrin transmembrane function. *Science* **267,** 883–885.